Since January 2020 Elsevier has created a COVID-19 resource centre with free information in English and Mandarin on the novel coronavirus COVID-19. The COVID-19 resource centre is hosted on Elsevier Connect, the company's public news and information website.

International Immunopharmacology 99 (2021) 108004

Contents lists available at ScienceDirect

International Immunopharmacology

journal homepage: www.elsevier.com/locate/intimp

Safety of inhaled ivermectin as a repurposed direct drug for treatment of COVID-19: A preclinical tolerance study

Suzan M. Mansour [a,b], Rehab N. Shamma [c,*], Kawkab A. Ahmed [d], Nirmeen A. Sabry [e], Gamal Esmat [f], Azza A. Mahmoud [g], Amr Maged [g,h]

[a] Department of Pharmacology and Toxicology, Faculty of Pharmacy, Cairo University, Egypt
[b] Department of Pharmacology, Toxicology and Biochemistry, Faculty of Pharmacy, Future University in Egypt, Cairo, Egypt
[c] Department of Pharmaceutics and Industrial Pharmacy, Faculty of Pharmacy, Cairo University, Egypt
[d] Department of Pathology, Faculty of Veterinary Medicine, Cairo University, Egypt
[e] Department of Clinical Pharmacy, Faculty of Pharmacy, Cairo University, Egypt
[f] Department of Endemic Medicine and Hepatogastroenterology, Faculty of Medicine, Cairo University, Egypt
[g] Department of Pharmaceutics and Pharmaceutical Technology, Faculty of Pharmacy, Future University in Egypt, Cairo, Egypt
[h] Pharmaceutical Factory, Faculty of Pharmacy, Future University in Egypt, Cairo, Egypt

ARTICLE INFO

Keywords:
COVID-19
Ivermectin
Toxicity
Safety
Pulmonary delivery

ABSTRACT

Introduction: SARS-CoV-2 replication in cell cultures has been shown to be inhibited by ivermectin. However, ivermectin's low aqueous solubility and bioavailability hinders its application in COVID-19 treatment. Also, it has been suggested that best outcomes for this medication can be achieved *via* direct administration to the lung.
Objectives: This study aimed at evaluating the safety of a novel ivermectin inhalable formulation in rats as a preclinical step.
Methods: Hydroxy propyl-β-cyclodextrin (HP-β-CD) was used to formulate readily soluble ivermectin lyophilized powder. Adult male rats were used to test lung toxicity for ivermectin-HP-β-CD formulations in doses of 0.05, 0.1, 0.2, 0.4 and 0.8 mg/kg for 3 successive days.
Results: The X-ray diffraction for lyophilized ivermectin-HP-β-CD revealed its amorphous structure that increased drug aqueous solubility 127-fold and was rapidly dissolved within 5 s in saline. Pulmonary administration of ivermectin-HP-β-CD in doses of 0.2, 0.4 and 0.8 mg/kg showed dose-dependent increase in levels of TNF-α, IL-6, IL-13 and ICAM-1 as well as gene expression of MCP-1, protein expression of PIII-NP and serum levels of SP-D paralleled by reduction in IL-10. Moreover, lungs treated with ivermectin (0.2 mg/kg) revealed mild histopathological alterations, while severe pulmonary damage was seen in rats treated with ivermectin at doses of 0.4 and 0.8 mg/kg. However, ivermectin-HP-β-CD formulation administered in doses of 0.05 and 0.1 mg/kg revealed safety profiles.
Conclusion: The safety of inhaled ivermectin-HP-β-CD formulation is dose-dependent. Nevertheless, use of low doses (0.05 and 0.1 mg/kg) could be considered as a possible therapeutic regimen in COVID-19 cases.

1. Introduction

The COVID-19 pandemic is arguably the world's most serious health epidemic and the biggest threat since second World War. Currently, available protocols for managing COVID-19 patients depends mainly on supporting patients, alleviating symptoms and preventing respiratory and other organ failures. Although remdesivir, received Food and Drug Administration (FDA) authorization for treatment of hospitalized COVID-19 patients, there are currently no other specific therapies approved by the FDA [1] for this indication. Thus, the world is in great need of developing novel medications or repurposing (repositioning) of existing ones for other therapeutic application in order to develop safe and efficient treatments for COVID-19. Numerous previously available medications used as treatments for malaria (chloroquine and hydroxychloroquine) [2,3], SARS-CoV (lopinavir and ritonavir) [4,5], influenza viruses (favipiravir and oseltamivir) [6,7], virus C hepatitis (ribavirin and sofosbuvir) [8,9] and helminth/parasitic infections (ivermectin) were tested for treatment of COVID-19 [10,11].

* Corresponding author at: Faculty of Pharmacy, Cairo University, Cairo 11562, Egypt.
E-mail address: rehab.shamma@pharma.cu.edu.eg (R. N. Shamma).

https://doi.org/10.1016/j.intimp.2021.108004
Received 7 May 2021; Received in revised form 13 July 2021; Accepted 19 July 2021
Available online 23 July 2021

Ivermectin an FDA-approved antiparasitic drug that is used to treat several neglected tropical diseases, including onchocerciasis, helminthiases, and scabies [12,13] has demonstrated an excellent safety profile. Ivermectin is a mysterious multifaceted 'wonder' drug that keeps shocking and exceeding expectations [14]. It was repositioned as cancer drug [15,16] and showed potent antiviral activity against Zika [17], HIV-1 and dengue [18] viruses. Ivermectin was reported to inhibit the replication of SARS-CoV-2 in cell cultures [19] possibly through an RNA-dependent RNA polymerase (RdRp)-ivermectin complex, which is recognized as the most possible target for the in-vitro anti SARS-CoV-2 activity of ivermectin [20], thus inhibiting coronavirus replication and transcription inside the host cell [21]. Noteworthy, available pharmacokinetic data from clinically relevant and excessive dosing studies indicate that the SARS-CoV-2 inhibitory concentrations for ivermectin are much argued. Some authors reported that effective concentrations are not likely attainable in humans [22] and suggested that the required plasma concentrations necessary for the antiviral efficacy as detected *in-vitro* requires the administration of 100-fold the doses approved for use in humans [23,24] due to its poor solubility [25] and bioavailability [26]. While others reported that ivermectin achieves lung concentrations over 10-fold higher than its reported EC50 [27]. Despite the fact that ivermectin tends to accumulate in lung tissue, expected systemic plasma and lung tissue concentrations are much lower than the *in-vitro* calculated half-maximal inhibitory concentration (IC50) against SARS-CoV-2 (~2 μM) [28]. SARS-CoV-2-induced lung inflammation or injury could further greatly affect the ability of ivermectin to accumulate in the lung cells due to changes in the pulmonary microenvironment by inflammation provoked alterations in body temperature, enzymatic activity, and pH [29]. Hence, the advantages of lung accumulation for ivermectin may be hampered during treatment of severe SARS-CoV-2 infection

Furthermore, ivermectin neurotoxicity has been raised by Chaccour *et al.*, especially in patients with COVID-19-induced hyperinflammation. Furthermore, drug interactions with potent CYP3A4 inhibitors (such as ritonavir) necessitate careful evaluation of co-administered medications. Finally, evidence indicates that achieving significant ivermectin plasma levels with COVID-19 activity would necessitate potentially toxic rises in ivermectin doses in humans [23].

Local ivermectin administration directly to the lung may represent a potential approach for the difficulties caused by the multiple biological barriers that encountered in the drug delivery. Over the past two decades, pulmonary drug delivery has gained much interest, offering an interesting route having several advantages over other drug delivery routes including high drug-loading efficiency, and enhanced absorption to the lung epithelium making the inhalation route an ideal drug delivery approach [30].

Many pharmaceutical researchers are interested in cyclodextrin (CD) complexation as its effectiveness has been demonstrated in improving the solubility, stability, and bioavailability of a variety of lipophilic active compounds [31–36]. CDs can form stable complexes with protein hydrophobic moieties that are vulnerable to aggregation, participate in hydrogen bonding with proteins, and have an intrinsic surfactant-like effect [37]. Researchers investigated the possibility of using CDs to improve the solubility of non-polar medications for inhalation therapy. The superiority of hydroxy propyl-β-cyclodextrin (HP-β-CD) over other CD derivatives has been clearly identified, and it has been documented to actually demonstrate surface-active properties that are needed for effective protein surface protection through spray freeze-drying [38–40].

HP-β-CD was used to formulate inhaled dry powder for salbutamol, and results confirmed the successful application of CDs in promoting lung delivery of drugs [41]. Furthermore, Guan *et al.,* reported the successful use of naringenin-HP-β-CD inhalation solution for nebulization to achieve a rapid response with reduced dose for the treatment of cough [42]. Milani *et al.,* reported the ability to enhance the stability and aerosolization for the freeze-dried IgG formulation using HP-β-CD which acted as water-replacement agent or a surfactant [43]. The use of HP-β-CD in the treatment of chronic obstructive pulmonary disease has been reported *via* the inhalation route, owing to its ability to decrease the production of CXCL-1, a potent chemotactic agent for neutrophils in various inflammatory conditions and LPS-induced peribronchial inflammation [44].

The lyophilization process is used to remove the frozen solvent from a sample by sublimation, which involves freezing and then drying the sample at low temperature and pressure [45]. Lyophilization is a pivotal drying process for pharmaceutical and biopharmaceutical products because such process is energy efficiency, scalable and lyophilized finished product has low residual water content [46]. Over the last five years, the use of lyophilization for both pharmaceutical and biopharmaceutical development has increased by approximately 13.5 percent per year [47]. The freeze-drying method is adaptable, cost-effective, and simple to scale up. It's good for heat- and water-labile drugs, and it is supposed to be useful for changing the physicochemical properties of hydrophobic drugs. Furthermore, Doile *et al.,* evaluated different methods in the preparation of inclusion complexes with β-CD; namely, kneading, co-evaporation and freeze drying. Their results confirmed the superiority of the freeze drying technique in improving the dissolution rate of the poorly water soluble drug, dexamethasone acetate [48].

The suggested ivermectin doses in treatment of COVID-19 is very high and this can increase its incidence of side effects. This problem can be solved by delivering ivermectin to the lung tissue by inhalation. The solubility of ivermectin should be enhanced in such delivery system to increase its bioavailability. In March 2021, and based on the WHO, the decision to use the ivermectin in COVID-19 patients was inconclusive and the WHO recommended that the drug can be used within clinical trials [49]. Therefore, in this proposed work, ivermectin lyophilized formulation was developed using hydroxy propyl-β-cyclodextrin as a carrier. The safety of the proposed formulation on lung tissue was tested in male Wistar rats using histopathological and biological evaluations.

2. Materials and methods

2.1. Drugs and chemicals

Ivermectin was kindly provided by EgyEuro Animal Health Company, Egypt and it was originally purchased from North China Pharma Group Aino, China with technical purity of 97%. Hydroxy propyl-β-cyclodextrin (HP-β-CD) was kindly donated by Roquette, France. Tween 80 was purchased from El-Nasr Pharmaceutical Chemicals (Egypt).

2.2. Animals

Adult male Wistar rats weighing 200 to 220 g were obtained from the National Research Centre's breeding colony (NRC, Giza, Egypt). Before beginning any experimental procedure, animals were required to acclimate for one week in the animal facility of the Faculty of Pharmacy (Cairo University, Egypt). Under a 12:12 light–dark cycle, the rats were given unlimited water and a normal laboratory diet. This work was undertaken in strict accordance to the recommendations of the Guide for the Care and Use of Laboratory Animals of the National Institutes of Health. The protocol was approved by the Research Ethics Committee of the Faculty of Pharmacy, Cairo University, Cairo, Egypt (PT-2968; 26/04/2021). All procedures were performed under thiopental sodium (50 mg/kg, i.p.) anesthesia.

2.3. Preparation of ivermectin formulation

Briefly, ivermectin was dissolved in distilled water in the presence of HP-β-CD as carrier (1:200 wt ratio) to enhance ivermectin solubility. Furthermore, 0.02 w/v% Tween 80 was added to the solution. The prepared solution was frozen overnight at -80 °C, then the frozen

solution was lyophilized in a Christ freeze dryer (ALPHA 2–4 LD plus, Germany) under a temperature of -80 °C and vacuum of 7×10^{-2} mbar for 24 h. After the freeze-drying process, the dried powder was collected and stored in a tightly closed container.

2.4. Determination of ivermectin solubility

The solubility of the lyophilized ivermectin formulation was compared with the solubility for the drug alone and the formulation physical mixture. The samples were added in excess amounts in well-closed vials containing 3 mL of normal saline solution (reconstitution media for lung delivery). The samples were agitated at room temperature for 72 h using an incubator shaker (IKA KS 4000, Germany). After reaching an equilibrium where the solubility became constant, the samples were filtered using cellulose membrane syringe filter with a pore size of 0.2 μm (Chmlab Group, Spain) to remove the insoluble ivermectin. After filtration, the samples were measured for drug concentration using an ultraviolet spectrophotometer (Shimadzu Spectrophotometer UV-1800, Japan) at 245 nm.

2.5. Reconstitution test

The reconstitution study of the lyophilized ivermectin formulation was performed in normal saline (reconstitution media for lung delivery). A proper amount of powder (200 mg) equivalent to 1 mg of ivermectin was added into vials containing 3 mL normal saline solution and shaken well for the reconstitution. Images were taken at different times to observe the reconstitution process using a digital camera (Nikon D5200, Japan).

2.6. Powder X-ray diffraction (XRD)

The crystalline structure of ivermectin pure powder, HP-β-CD, physical mixture, and lyophilized ivermectin formulation, in addition to its corresponding non-medicated formulation were examined in a Scintag X-ray diffractometer (USA) using Cu-radiation with a nickel filter at a voltage of 45 kV, a current of 40 mA and scanning speed of 0.02°/sec. The reflection peaks between $2\theta = 2°$ and 80°, the corresponding spacing (d, A°) were determined using HighScore Plus, Malvern Panalytical Ltd, UK and the relative intensities (I/I°) were determined by calculating the ratio between the height of a selected peak in the X-ray diffractogram in the lyophilized formulation (I) and its height in ivermectin diffractogram (I°) [50]

2.7. Lung toxicity study protocol

Forty-two animals were randomly and equally allocated into seven groups as follows; saline (S), non-medicated cyclodextrin formulation (Cd) and ivermectin formulations ($I_{0.05}$, $I_{0.1}$, $I_{0.2}$, $I_{0.4}$ and $I_{0.8}$) administered the lyophilized ivermectin-cyclodextrin formula reconstituted in saline in doses of 0.05, 0.1, 0.2, 0.4 and 0.8 mg/kg, respectively for 3 successive days. These doses were selected based on the approved oral doses in human. Ivermectin was given to rats after conversion of its human equivalent doses according to the formula of Phillips [Human dose normalized to body mass (μg/kg) = Animal drug dose per unit body mass (μg/kg)*(Animal body mass (kg)/ Human body mass (kg))^(1− constant) where 0.67 as the constant] [51]. Rats were anaesthetized with thiopental (50 mg/kg; ip) and the concentrations were adjusted so that each animal received 0.1 mL of the solution by intratracheal instillation. All rats were weighed daily, and by the end of the experiment (day 4), rats were deeply anaesthetized by an overdose of thiopental. Blood samples were obtained from the heart after chest opening. Sera were separated for the estimation of surfactant protein-D (SP-D) using the corresponding rat ELISA kit and both lungs were quickly harvested. The left lung tissue was preserved in 10% formalin in saline for histological investigation, while the right lung tissue was sectioned into parts and stored at - 80 °C until assessed next for the chosen biochemical parameters using the respective western blot, PCR, or ELISA methods.

2.7.1. Quantification of serum level of SP-D and lung contents of TNF-α, IL-6, IL-13, IL-10 and ICAM-1

Serum levels of pulmonary surfactant protein-D (SP-D, MBS703468) as well as lung contents of tumor necrosis factor-α (TNF-α, MBS2507393), interleukin-6 (IL-6, MBS175908), interleukin-13 (IL-13, MBS355408), interleukin-10 (IL-10, MBS034393) and intracellular adhesion molecule-1 (ICAM, MBS267983) were determined using their respective ELISA kits (MybioSource, CA, USA) according to the manufacturers' guidelines.

2.7.2. Assessment of the protein expression of procollagen III N-terminal propeptide (PIII-NP)

For assessment of the protein expression of procollagen III N-terminal propeptide (PIII-NP), the western blot method was used [52]. Briefly, lung tissues were homogenized in phosphate buffered saline. Then, 10 μg protein from each lung sample was separated using the SDS polyacrylamide gel electrophoresis and transferred to a nitrocellulose membrane. The nitrocellulose membrane was incubated with the anti-PIII-NP antibody (MBS2120628, (MybioSource, CA, USA) overnight at 4℃ and the formed blot was detected using enhanced chemiluminescence detection reagent (Amersham Biosciences, IL, USA). Results were expressed as arbitrary units against β-actin using image analysis software (Image J, version 1.46a, NIH, Bethesda, MD, USA).

2.7.3. Estimation of the gene expression monocyte chemoattractant protein-1 (MCP-1)

Gene expression of monocyte chemoattractant protein-1 (MCP-1) was estimated using the qRT-PCR technique. Following total RNA extraction (Invitrogen Life Technologies, Inc, CA, USA), Mx3000P real-time PCR system was used for the qRT-PCR (Stratagene, La Jolla, CA, USA) with two-phase program including 2 min at 50 °C, 10 min at 95 °C, 40 cycles of 15 s at 95 °C and 1 min at 60 °C. Each sample was examined in duplicate. Relative gene expression was calculated using the 2-ΔΔCt method. The primer sequences used for MCP-1 and the reference gene, β-actin, are listed in Table 1.

2.7.4. Histopathological examination of lungs

Lungs were removed and fixed in 10% formalin in saline for 72 h. All specimens were then washed, dehydrated, cleared and embedded in paraffin. The paraffin embedded blocks were sectioned at 5 μm thickness and stained with haematoxylin and eosin (H&E) for light microscopic examination (Olympus BX50, Tokyo, Japan) [53]. A blinded pathologist scored the pulmonary histopathological changes in the experimental groups using a scoring scale from 0 to 4 for each lung damage parameter (congestion, edema, hemorrhage, thickening of interalveolar septa and inflammatory cell infiltration) in five microscopic fields per section/rat (100x total magnification) [54].

2.8. Statistical analysis

The parametric data were expressed as means ± standard deviations (SD) and analyzed using the one-way analysis of variance (ANOVA) test followed by Tukey's Multiple Comparison test. The non-parametric data

Table 1
Primer sequences of the assessed genes.

Gene	Sequences
MCP-1	Forward 5′-CTGCTGCTACTCATTCACTGG-3′ Reverse 5′-TCTGTCATACTGGTCACTTCTACA-3′
β-Actin	Forward 5′-TTGTAACCAACTGGGACGATATGG-3′ Reverse 5′-GATCT TGATCT TCATGGTGCTAGG-3′

(scores) were interpreted as medians and analyzed using the non-parametric ANOVA Kruskal Wallis test, followed by the post-hoc Dunn's test. The GraphPad Prism1 software package for windows, version 7 (GraphPad Software Inc., CA, USA) was used to carry out all statistical tests and drawings. For all statistical procedures, the degree of significance was held at $p < 0.05$.

3. Results

3.1. Determination of ivermectin solubility and reconstitution time

Ivermectin's solubility changed when incorporated in the physical mixture or the lyophilized form (0.0047 ± 0.0004, 0.1431 ± 0.0070, 0.6005 ± 0.0120 mg/mL, respectively). The reconstitution property of the lyophilized powder was evaluated by the addition of 3 mL of normal saline solution in vials containing 200 mg powder. Fig. 1 demonstrats the rapid dissolution of the lyophilized formulation after 5 s of adding the normal saline solution. The lyophilized solution's clarity was compared with the deionized water, which did not show any turbidity or drug crystallization, owing to the high solubility of the lyophilized powder in water, as previously mentioned.

3.2. Powder X-ray diffraction

The physical form was evaluated using powder X-ray diffraction for the pure drug, HP-β-CD, formulation physical mixture, non-medicated lyophilized formulation, and the prepared medicated lyophilized formulation (Fig. 2) in the range from 2 to 80° 2θ. Two prominent diffraction peaks revealed in the X-ray diffractogram indicating the drug's crystalline nature at 2θ of 9.31°, and 13.09°.

Due to the amorphous nature for HP-β-CD, X-ray diffraction pattern showed low intensities broad and diffused peaks. When the ivermectin and HP-β-CD were physically blended, their diffractogram revealed their combined diffraction patterns. Meanwhile, the physical mixture's diffraction peak intensity decreased, possibly due to powder dilution. The intense characteristic peaks for the crystalline structure for ivermectin were not detected in the diffraction pattern of ivermectin-HP-β-CD lyophilized formulation, but instead, a typical diffuse pattern as that for HP-β-CD was detected. The absence of characteristic ivermectin diffraction peaks, indicates effective transformation into an amorphous state.

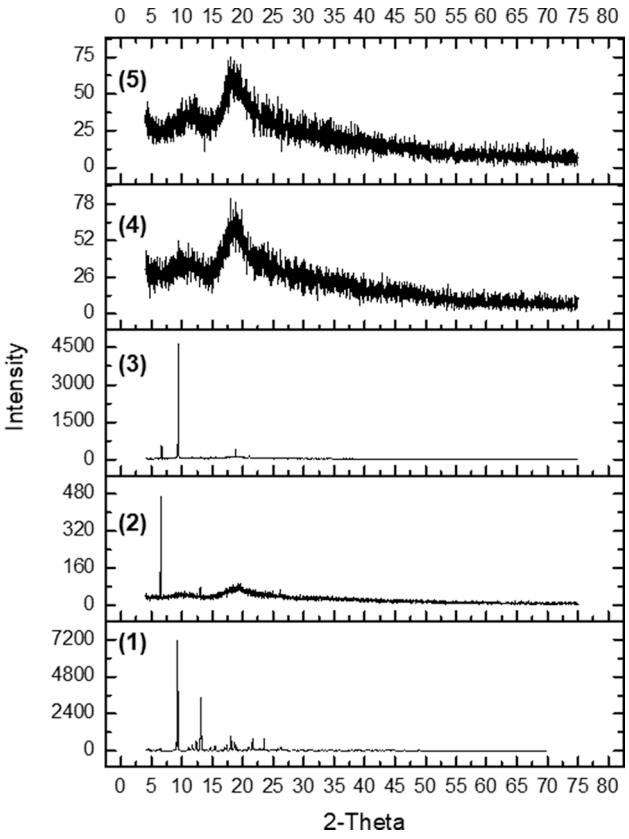

Fig. 2. X-ray diffraction pattern for: (1) ivermectin, (2) HP-β-CD, (3) physical mixture for ivermectin with HP-β-CD, (4) non-medicated formulation and (5) medicated formulation.

To evaluate the relative degree of crystallinity (RDC), pure drug peak at 2θ-value of 9.31 (I°) was used for calculating the RDC. The calculated RDC-values were 0.647, and 0.003, for the formulation physical mixture, and lyophilized formulation, respectively.

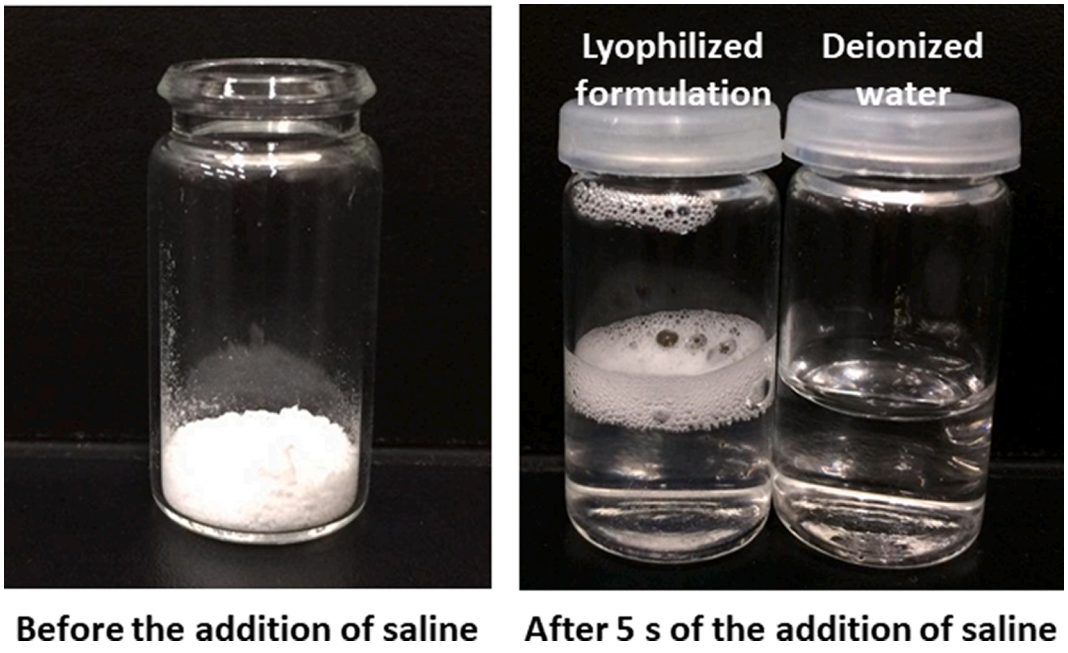

Fig. 1. Reconstitution images of the lyophilized powder before and after the addition of normal saline.

3.3. Biochemical studies

Since all findings showed no statistical significance among the normal-control group in which the animals received saline (S) and those receiving the non-medicated cyclodextrin formulation (Cd), all comparisons were conducted against the Cd group.

3.3.1. Effect of ivermectin inhalation on the inflammatory and anti-inflammatory pulmonary cytokines levels

As depicted in Fig. 3, intratracheal administration of ivermectin at doses of 0.05 and 0.1 mg/kg did not result in any significant alteration in the pulmonary contents of the inflammatory cytokines **(a)** TNF-α, **(b)** IL-6 and **(c)** IL-13 as compared to Cd group. However, inhaled ivermectin at dose of 0.1 mg/kg has markedly declined levels of the anti-inflammatory molecule **(d)** IL-10 as compared to Cd group. In a comparable manner, starting from the ivermectin dose of 0.2 mg/kg, a profound dose-dependent increase in the levels of the inflammatory cytokines namely, TNF-α, IL-6 and IL-13 paralleled by a profound reduction in the anti-inflammatory IL-10 was distinguished.

3.3.2. Effect of intratracheal administration of ivermectin on lung contents of ICAM-1 and the gene expression of MCP-1

As shown in Fig. 4**,** intratracheal administration of ivermectin at doses of 0.05 and 0.1 mg/kg for 3 consecutive days was not accompanied by any change in the pulmonary contents of the adhesion molecule, **(a)** ICAM-1 and the relative gene expression of **(b)** MCP-1 as compared to Cd group. In contrast, there were significant upshots in the lung contents of ICAM-1 and the gene expression of MCP-1 starting from ivermectin dose of 0.2 mg/kg and continued to reach 5.2 and 3.9-folds, respectively in ivermectin dose of 0.8 mg/kg as compared to Cd group.

3.3.3. Effect of intratracheal administration of ivermectin on pulmonary protein expression of PIII-NP and serum levels of SP-D

Intratracheal administration of ivermectin at doses of 0.05 and 0.1 mg/kg as demonstrated in Fig. 5**,** did not result in any marked change in the lung relative protein expression of the early profibrotic molecule, **(a)** PIII-NP, as well as the serum levels of acute lung injury biomarker, **(b)** SP-D as compared to the Cd group. On the contrary, inhaled ivermectin in doses of 0.2 – 0.8 mg/kg significantly increased the pulmonary protein expression of PIII-NP, as well as the serum levels of SP-D as compared to Cd group.

3.3.4. Effect of intratracheal administration of ivermectin on lung histological architecture

As illustrated in Fig. 6**,** lungs of **(a)** normal-control rats (S) revealed the normal histological lung architecture, normal alveoli, bronchioles and thin interalveolar septa. Similar observations were noticed in groups received **(b)** non-medicated formula (Cd), **(c and d)** ivermectin with

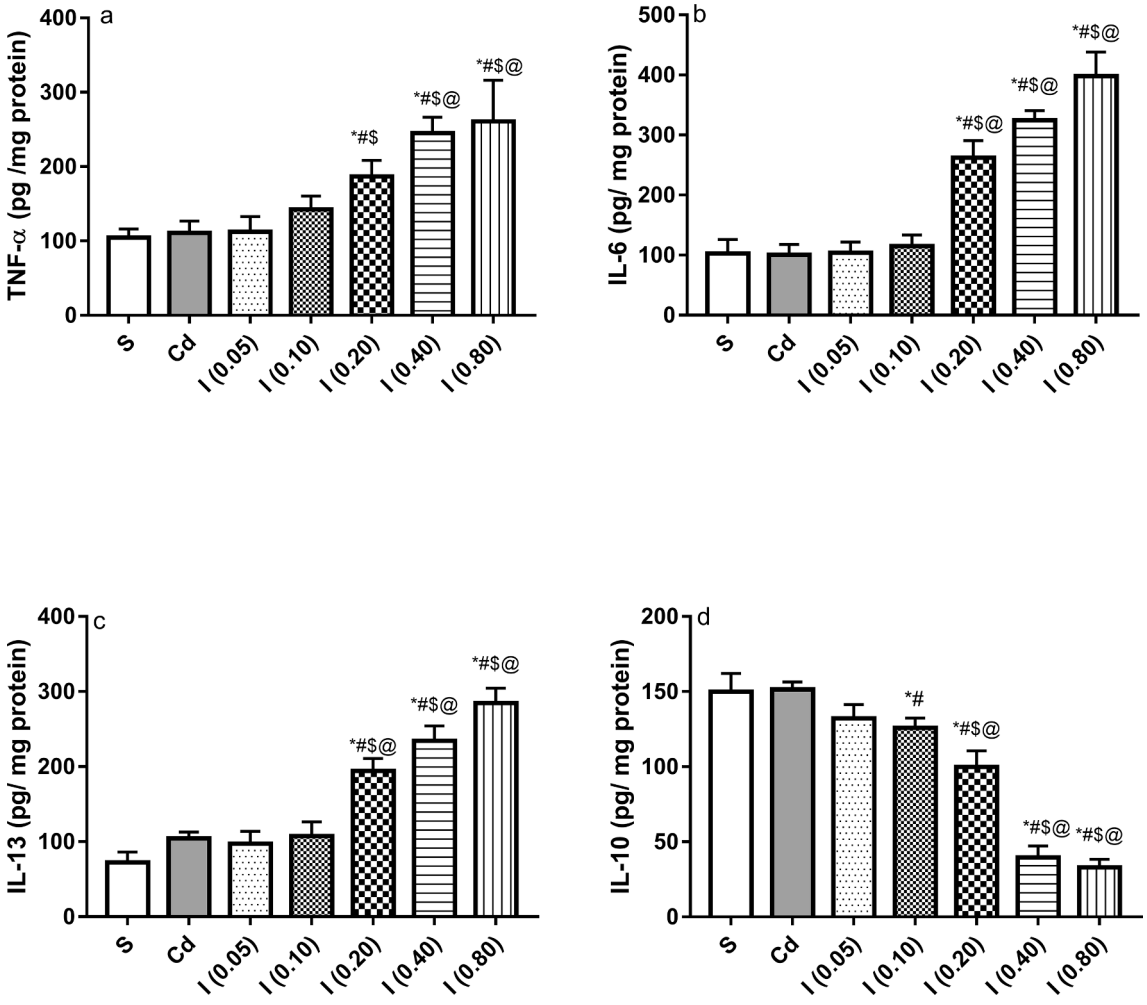

Fig. 3. Effect of intratracheal administration of ivermectin on lung (a) TNF-α, (b) IL-6, (c) IL-13 and (d) IL-10 contents. Data are presented as mean ± SD (n = 6). As significantly different from (*) S, (#) Cd, ($) $I_{0.05}$ and (@) $I_{0.1}$ groups, using one-way ANOVA followed by Tukey's post-hoc test ($p < 0.05$). S: saline, Cd: cyclodextrin, $I_{0.05}$, $I_{0.1}$, $I_{0.2}$, $I_{0.4}$, $I_{0.8}$: ivermectin (0.05, 0.1, 0.2, 0.4. 0.8 mg/kg, respectively), TNF-α: tumor necrosis factor-α, IL-6: interleukin-6, IL-13: interleukin-13 and IL-10: interleukin-10.

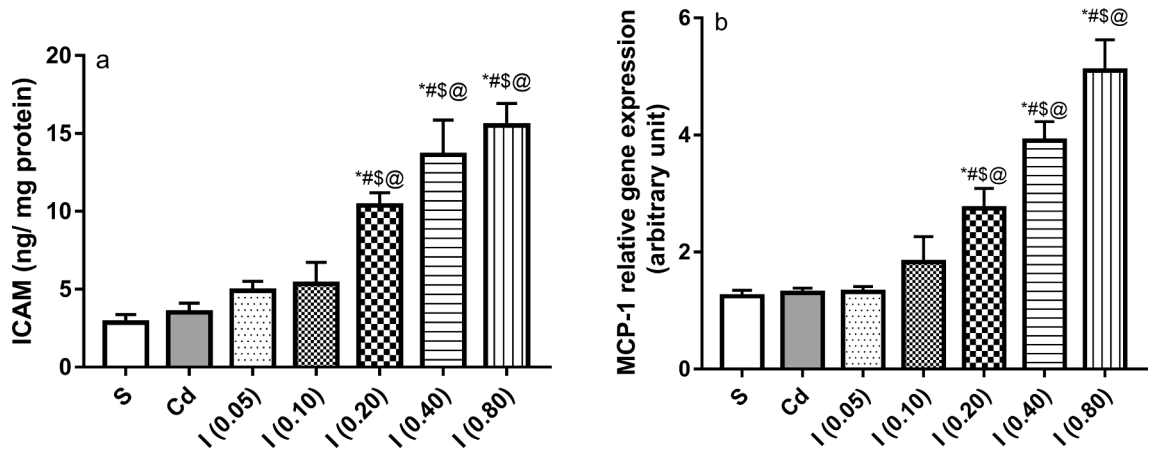

Fig. 4. Effect of intratracheal administration of ivermectin on lung (a) ICAM-1 content and (b) MCP-1 relative gene expression. Data are presented as mean ± SD (n = 6). As significantly different from (*) S, (#) Cd, ($) $I_{0.05}$ and (@) $I_{0.1}$ groups, using one-way ANOVA followed by Tukey's post-hoc test ($p < 0.05$). S: saline, Cd: cyclodextrin, $I_{0.05,}$ $I_{0.1,}$ $I_{0.2,}$ $I_{0.4,}$ $I_{0.8}$: ivermectin (0.05, 0.1, 0.2, 0.4. 0.8 mg/kg, respectively), ICAM-1: intracellular adhesion molecule-1, MCP-1: monocyte chemoattractant protein-1.

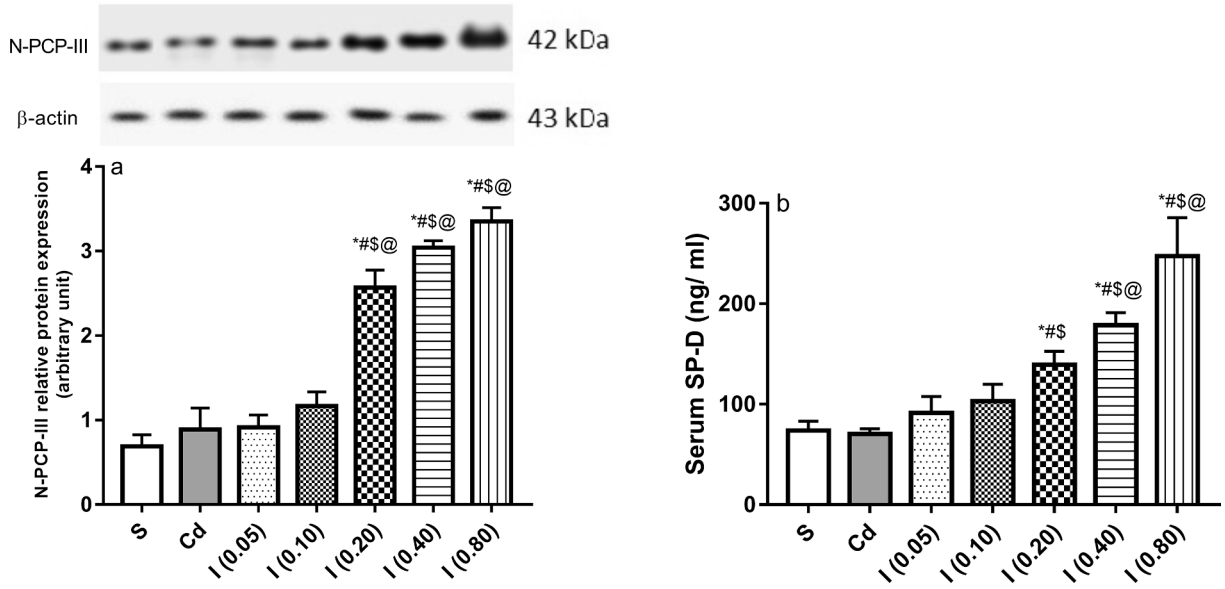

Fig. 5. Effect of intratracheal administration of ivermectin on lung relative protein expression of (a) PIII-NP and serum levels of (b) SP-D. Data are presented as mean ± SD (n = 6). As significantly different from (*) S, (#) Cd, ($) $I_{0.05}$ and (@) $I_{0.1}$ groups, using one-way ANOVA followed by Tukey's post-hoc test ($p < 0.05$). S: saline, Cd: cyclodextrin, $I_{0.05,}$ $I_{0.1,}$ $I_{0.2,}$ $I_{0.4,}$ $I_{0.8}$: ivermectin (0.05, 0.1, 0.2, 0.4. 0.8 mg/kg, respectively), PIII-NP: procollagen III N-terminal propeptide and SP-D: surfactant protein-D.

doses of 0.05 and 0.1 mg/kg ($I_{0.05}$ and $I_{0.1}$, respectively). However, lungs of rats treated with **(e and f)** ivermectin in a dose of 0.2 mg/kg ($I_{0.2}$) revealed mild histopathological alterations with slight focal thickening of the interalveolar septa and perivascular few inflammatory cells infiltration. Furthermore, severe pulmonary damage was seen in examined sections from rats treated with ivermectin dose of 0.4 mg/kg ($I_{0.4}$) with **(g)** marked interalveolar septa thickening with inflammatory cells, **(h)** edema in the interlobular septa associated with inflammatory infiltrate, as well as focal aggregations of inflammatory cells in **(h)** lymphocytes and **(i)** macrophages. Similarly, lungs of rats treated with 0.8 mg/kg ivermectin ($I_{0.8}$) exhibited more severe histopathological alterations demonstrated as **(j)** congestion of pulmonary blood vessels and focal hemorrhage, **(j and k)** marked thickening of interalveolar septa with inflammatory cells and **(l)** multifocal aggregations of inflammatory cells (mainly lymphocytes and macrophages) associated with perivascular inflammatory cells infiltration. These data are summarized as scoring of the collective and individual structural changes in panels **m** and **n**, respectively.

4. Discussion

The usage of ivermectin in the management of COVID-19 is controversial. Literature existing pharmacokinetic and pharmacodynamic data show that SARS-CoV-2 inhibitory concentrations for ivermectin are not possibly achievable in humans due to its poor solubility and bioavailability [55–57]. Hence, its use in higher doses may be associated with many systemic adverse events. The present work aimed, on one hand, to prepare a HP-β-CD lyophilized readily soluble ivermectin formulation and, on the other hand, to assess the effect of intratracheal administration of this formulation on biochemical and histopathological changes in the lungs. It is postulated that ivermectin inhaled formulation is effective in SARS-CoV-2 infections. Hence, assessment of the risk–benefit profile of inhaled ivermectin is obliged [58].

Ivermectin is classified according to biopharmaceutical classification

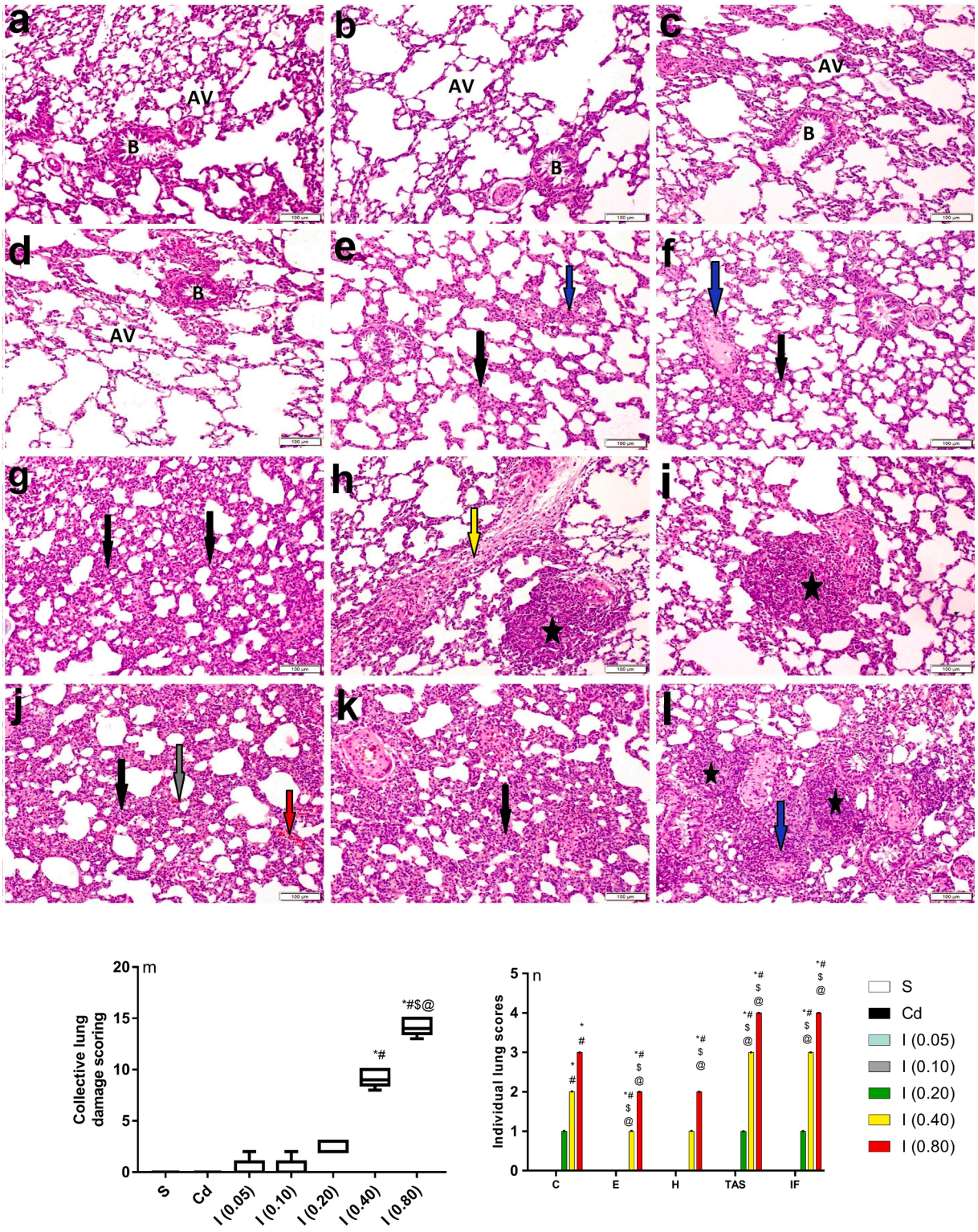

Fig. 6. Photomicrographs of lungs in ivermectin-treated rats (H&E; 200X). Sections of **(a)** normal control (S) group showing normal histological architecture of lung parenchyma with normal alveoli (AV) and bronchioles (B). Sections of **(b)** non-medicated (Cd), **(c)** $I_{0.05}$ and **(d)** $I_{0.1}$ demonstrating no histopathological alterations. Sections of **(e & f)** $I_{0.2}$, **(g, h & i)** $I_{0.4}$ and **(j, k & l)** $I_{0.8}$ representing thickening of interalveolar septa with inflammatory cells *(black arrow)*, perivascular inflammatory cells infiltration *(blue arrow)*, interlobular edema *(yellow arrow)*, congestion of pulmonary blood vessel *(red arrow)*, hemorrhage *(grey arrow)* and focal inflammatory cells aggregation *(asterisk)* (scale bar = 100 μm). Panels **m** and **n** summarize scoring of the collective and individual changes of 5 randomly chosen non-overlapping fields, respectively using Kruskal-Wallis followed by Dunn's multiple comparisons test ($p < 0.05$). S: saline, Cd: cyclodextrin, $I_{0.05}$, $I_{0.1}$, $I_{0.2}$, $I_{0.4}$, $I_{0.8}$: ivermectin (0.05, 0.1, 0.2, 0.4. 0.8 mg/kg, respectively), C: congestion, E: edema, H: hemorrhage, TAS: thickening of interalveolar septa, IF: inflammatory cells infiltration.

system (BCS) as class 4/3 drug, which is practically insoluble in water and has low permeability [59]. The prepared lyophilized ivermectin formulation showed 127-fold increase in drug solubility than the drug alone ($p < 0.05$). The enhancement of solubility is attributed to the complexation of the drug with the hydrophobic cavity of HP-β-CD, which increases the drug aqueous solubility [60,61]. HP-β-CD molecule has primary, and secondary hydroxyl groups located on the narrow rim and wider rim of the molecule [62], respectively, responsible for its hydrophilicity [63]. Due to its hydrophilic outer surface and large number of hydrogen bond donors and acceptors, HP-β-CD can form hydrogen bonds with several drugs. Furthermore, ivermectin molecule has several exposed hydroxyl and ester groups [55), which can act as a hydrogen bond donor with the hydroxyl groups in HP-β-CD to form complex. HP-β-CD was chosen for this study because of its high water solubility (50 times greater than β-CD), low parenteral toxicity, and high biocompatibility and pharmacological inactivity, allowing it to be administered parenterally, orally, ophthalmically, and by inhalation [64]. Wang *et al.,* presented a novel approach for complexing hydrophobic drugs as Ketoprofen and nitrendipine with HP-β-CD using lyophilization [60].

On the other hand, the drug in lyophilized form revealed 4-fold increase in drug solubility than the drug in a physical mixture ($p < 0.05$). This can be explained by the fact that, HP-β-CD in physical mixture acts only to decrease the interfacial tension between the drug and the aqueous medium, while the lyophilization process results in a complete inclusion complex with the drug and increases the aqueous solubility [65]. This improved solubility of the lyophilized powder is necessary for rapid reconstitution in aqueous media before use.

The rapid reconstitution and solubility of the lyophilized formulation are attributed to the amorphous complexation of the drug with HP-β-CD, which confirmed the results obtained by the X-ray diffraction study. Vass and his team formulated a reconstitution dosage form of voriconazole with HP-β-CD using an electrospinning process. The prepared complex showed complete reconstitution and a clear solution after 30 s of vigorous shaking [66].

Ivermectin has a high melting point (155 °C), indicating strong crystal lattice energy, which contributes to its poor aqueous solubility [50]. The incorporation of the drug into the cavity of a cyclodextrin molecule will cause the drug's crystalline nature to be disrupted, resulting in the formation of an inclusion complex. This causes a partial or complete loss of drug's crystallinity, which leads to an increase in its solubility. Inclusion complex formation typically causes noticeable changes in X-ray diffraction patterns of molecules, such as amorphization and the absence of the drug's characteristic peaks. The characteristic diffraction peaks of ivermectin were still detected in the physical mixture. However, they were significantly lowered in the corresponding medicated formulation, indicating a greater amorphousness of the prepared medicated formulation, compared to the plain drug [67]. This is indicative that the inclusion compound was formed in the lyophilization process and explains the results of improvement in ivermectin solubility and the fast reconstitution of the lyophilized powder. Similar results were obtained by Ammar *et al.* in their study on enhancing the solubility of glimepiride through the formation of inclusion complex with cyclodextrins [68]. The mechanism responsible for the precipitation of amorphous form was proposed that the presence of HP-β-CD inhibited solution-mediated crystallization occurring at the initial step of "Ostwald's Rule of Stages.". It can be concluded that ivermectin was molecularly well dispersed in the matrix of HP-β-CD, and amorphous ivermectin was formed [69]. Also, this new amorphous form is related to finite-size effects, preventing the drug molecules from rearranging themselves in a crystal lattice [70].

Apart from the improved solubility profile of the HP-β-CD lyophilized ivermectin formulation, the findings of the current work showed that intratracheal administration of such formulation loaded with different doses (allometric scaling) of ivermectin for three consecutive days, indeed, was accompanied by biochemical and histopathological changes in the lungs of male Wistar rats. These effects could be summarized as inflammation, profibrotic state, as well as distorted pulmonary histological architecture, that started from moderate dose of ivermectin (0.2 mg/kg/day) and escalated up to the higher dose (0.8 mg/kg/day). However, lower doses of ivermectin namely, 0.05 and 0.01 mg/kg were not accompanied by any biochemical or histological changes.

Re-positioning of drugs for the management of COVID-19 is an ultimate approach, however, it is only possible if the safety of the drug has been proved at the dose levels that are effective. Intratracheal administration of ivermectin at different human equivalent doses *viz;* 0.2, 0.4 and 0.8 mg/kg for 3 successive days was accompanied by pronounced pulmonary inflammation as evidenced by the increased lung proinflammatory cytokines contents namely, TNF-α, IL-6 and IL-13, paralleled by reduction in the levels of the anti-inflammatory molecule, IL-10. These effects were obvious from the dose of 0.2 mg/kg and up-surged till the 0.8 mg/kg dose level. These molecular events were corroborated with the histopathological results as manifested by inflammatory infiltration and focal aggregations of lymphocytes and macrophages. Such changes were reflected as raised serum levels of SP-D, a marker for acute lung injury.

Only few data are available about the safety of inhaled ivermectin formulation. A study by Chaccour *et al.* reported no adverse events on rats following the administration of various doses of nebulized ivermectin alcoholic solution (lower dose of 80–90 mg/kg and higher dose of 110–140 mg/kg), that contradicts with what observed herein [57]. On the other hand, these molecular and histological alterations observed with the higher doses level in our study were not detected in the lower ones *viz,* 0.1 and 0.2 mg/kg.

Increased pulmonary inflammatory cytokines levels are documented in several cases of lung injury [71–73]. The proinflammatory M1 macrophages mature in response to variety of factors including interferon, lipopolysaccharide, high-mobility group protein or other cytokines e.g., TNF-α. The activated M1 macrophages further release proinflammatory cytokines involving TNF-α and IL-6 as observed herein and create cytotoxic oxidant stress and proteolytic states [73]. Although the acute lung injury and tenacious inflammation include a delayed or exacerbated reaction of M1 macrophages and faulty M2 macrophage-induced lung repair, the advancement of ongoing illnesses such as fibrosis and cancer are believed to be an outcome of increased production of IL-4 and IL-13 by the hyper-responsive subpopulations of M2 macrophages [74]. Facts that may explain, at least in part, the observed rise in IL-13 pulmonary content following ivermectin intratracheal instillation. IL-13 is a double-edged sword where it possesses both anti-inflammatory and proinflammatory effects. It may induce tissue resident macrophages to develop into profibrotic-activated macrophages that are involved in the fibrotic responses induced by infections [75], and bleomycin [76] with buildup of cytokines and growth factors such as transforming growth factor-β during both the pulmonary repair and fibrotic phases following the acute inflammatory stage [52]. Accordingly, it can be assumed that greater doses of ivermectin might result in serious alterations in the lung tissue that may overcome its beneficial antiviral activity against SARS-CoV-2.

The mutual crosstalk between aggravated pulmonary inflammation and fibrosis has been also pinned down here. Intratracheal instillation of ivermectin in doses of 0.2–0.8 mg/kg markedly enhanced the protein expression of the fibroproliferation marker, N-PCP-III, which goes in line with a previous report [77]. N-PCP-III is considered as an early response to lung injury [78] that liberated during the conversion of type-III procollagen to type-III collagen and correlates positively with the grade of pulmonary fibrosis [79]. Bejermer *et al.* showed that patients with idiopathic pulmonary fibrosis exhibited higher N-PCP-III levels with deteriorated lung function than those with stable disease [80]. These results were further supported as mentioned above by the elevated SP-D serum levels. Changes in SP-D structure and function have been involved in a wide assortment of pulmonary diseases. These

include pneumonia [81], acute respiratory distress syndrome [82], cystic fibrosis [83], and interstitial fibrosis [84].

Another important consequence for the exacerbated pulmonary inflammation is the TNF-α mediated stimulation of the cell surface glycoprotein, ICAM-1 [85,86] as observed herein following the administration of ivermectin in doses of 0.2 to 0.8 mg/kg. ICAM-1 performs a crucial role in the influx of neutrophils into the lung [87]. Increased levels of ICAM-1 have been noticed in cases of airway inflammation disorders and in many patients, ICAM-1 levels reflect the severity of the disease [88]. Furthermore, it was reported that ICAM-1 levels are positively correlated with increased pulmonary fibrosis [89]. To the authors knowledge, this is the first report examining the effect of ivermectin administration on ICAM-1 level.

The current investigation further demonstrated that intratracheal administration of ivermectin formulation in doses of 0.2 to 0.8 mg/kg was accompanied by an upshot in the gene expression of MCP-1, an important member of the chemokine family. MCP-1 is crucial in the development of inflammation [90]. Chronic and acute inflammation was reported to increase MCP-1 expression [91,92]. MCP-1 stimulates mononuclear cells, macrophages, and induces cytokine expression by binding to its major receptor—CCR2 [93], that may perpetuate the inflammatory process as aforementioned. In contradistinction, topical treatment with ivermectin in several skin infections was shown to reduce the levels of MCP-1 [94,95].

5. Conclusion

Ivermectin-hydroxy propyl-β-cyclodextrin lyophilized formulation was prepared in 1:200 wt ratio. The lyophilized ivermectin formulation showed 127 and 30-fold increase in drug solubility compared to drug alone and drug in the physical mixture, respectively. Ivermectin X-ray diffraction patterns changed from crystalline pattern for pure drug to amorphous pattern for lyophilized formulation which revealed fast dissolution of the lyophilized powder.

This study also demonstrated the safety of different doses of inhaled ivermectin formulation with recommendation that lower doses namely, 0.05 and 0.1 mg/kg can be used as a potential treatment for COVID-19. Moreover, the current work was the first to show the probable deleterious impacts of higher doses of inhaled ivermectin (0.2, 0.4 and 0.8 mg/kg) on the lungs. This could be partially attributed to increased inflammatory and profibrotic states, as well as distorted lung architecture. The value of ivermectin in COVID-19 cases, however, requires further investigations to prove its risk/benefit profile.

Declaration of Competing Interest

The authors declare that they have no known competing financial interests or personal relationships that could have appeared to influence the work reported in this paper.

References

[1] Centers for Disease Control and Prevention. Coronavirus (COVID-19): Get the Facts About Coronavirus. 2020 [cited 2020 6/9/2020]; Available from: https://www.cdc.gov/coronavirus/2019-ncov/index.html.

[2] S.A. Meo, D.C. Klonoff, J. Akram, Efficacy of chloroquine and hydroxychloroquine in the treatment of COVID-19, Eur. Rev. Med. Pharmacol. Sci. 24 (8) (2020 Apr) 4539–4547.

[3] S. Saqrane, M.A. El Mhammedi, Review on the global epidemiological situation and the efficacy of chloroquine and hydroxychloroquine for the treatment of COVID-19, New Microbes New Infect. 35 (2020 May), 100680.

[4] D. Dolan, J. Ingham, J. Baombe, BET 1: Lopinavir-ritonavir and COVID-19, Emerg. Med. J. 37 (7) (2020 Jul) 450–451.

[5] S. Meini, A. Pagotto, B. Longo, I. Vendramin, D. Pecori, C. Tascini, Role of Lopinavir/Ritonavir in the Treatment of Covid-19: A Review of Current Evidence, Guideline Recommendations, and Perspectives, J. Clin. Med. 9 (7) (2020). Jun 30.

[6] V. Pilkington, T. Pepperrell, A. Hill, A review of the safety of favipiravir - a potential treatment in the COVID-19 pandemic? J. Virus Erad. 6 (2) (2020 Apr 30) 45–51.

[7] J. Akram, S. Azhar, M. Shahzad, W. Latif, K.S. Khan, Pakistan Randomized and Observational Trial to Evaluate Coronavirus Treatment (PROTECT) of Hydroxychloroquine, Oseltamivir and Azithromycin to treat newly diagnosed patients with COVID-19 infection who have no comorbidities like diabetes mellitus: A structured summary of a study protocol for a randomized controlled trial, Trials. 21 (1) (2020 Aug 8) 702.

[8] G. Eslami, S. Mousaviasl, E. Radmanesh, S. Jelvay, S. Bitaraf, B. Simmons, et al., The impact of sofosbuvir/daclatasvir or ribavirin in patients with severe COVID-19, J. Antimicrob. Chemother. 19 (2020 Aug).

[9] H. Abbaspour Kasgari, S. Moradi, A.M. Shabani, F. Babamahmoodi, A.R. Davoudi Badabi, L. Davoudi, et al., Evaluation of the efficacy of sofosbuvir plus daclatasvir in combination with ribavirin for hospitalized COVID-19 patients with moderate disease compared with standard care: a single-centre, randomized controlled trial, J. Antimicrob. Chemother. 19 (2020 Aug).

[10] K. Sharun, K. Dhama, S.K. Patel, M. Pathak, R. Tiwari, B.R. Singh, et al., Ivermectin, a new candidate therapeutic against SARS-CoV-2/COVID-19, Ann Clin Microbiol Antimicrob. 19 (1) (2020 May 30) 23.

[11] F. Heidary, R. Gharebaghi, Ivermectin: a systematic review from antiviral effects to COVID-19 complementary regimen, J. Antibiot. (Tokyo) 73 (9) (2020 Sep) 593–602.

[12] A. Gonzalez Canga, A.M. Sahagun Prieto, M.J. Diez Liebana, N. Fernandez Martinez, M. Sierra Vega, J.J. Garcia Vieitez, The pharmacokinetics and interactions of ivermectin in humans–a mini-review, AAPS J. 10 (1) (2008) 42–46.

[13] S. Rosumeck, A. Nast, C. Dressler, Ivermectin and permethrin for treating scabies, Cochrane Database Syst. Rev. (2018). Apr 2;4:CD012994.

[14] A. Crump, Ivermectin: enigmatic multifaceted 'wonder' drug continues to surprise and exceed expectations, J. Antibiot. (Tokyo) 70 (5) (2017 May) 495–505.

[15] M. Juarez, A. Schcolnik-Cabrera, A. Duenas-Gonzalez, The multitargeted drug ivermectin: from an antiparasitic agent to a repositioned cancer drug, Am J Cancer Res. 8 (2) (2018) 317–331.

[16] A. Markowska, J. Kaysiewicz, J. Markowska, A. Huczynski, Doxycycline, salinomycin, monensin and ivermectin repositioned as cancer drugs, Bioorg. Med. Chem. Lett. 29 (13) (2019 Jul 1) 1549–1554.

[17] H. Ketkar, L. Yang, G.P. Wormser, P. Wang, Lack of efficacy of ivermectin for prevention of a lethal Zika virus infection in a murine system, Diagn. Microbiol. Infect. Dis. 95 (1) (2019 Sep) 38–40.

[18] K.M. Wagstaff, H. Sivakumaran, S.M. Heaton, D. Harrich, D.A. Jans, Ivermectin is a specific inhibitor of importin alpha/beta-mediated nuclear import able to inhibit replication of HIV-1 and dengue virus, Biochem. J. 443 (3) (2012 May 1) 851–856.

[19] L. Caly, J.D. Druce, M.G. Catton, D.A. Jans, K.M. Wagstaff, The FDA-approved drug ivermectin inhibits the replication of SARS-CoV-2 in vitro, Antiviral Res. 178 (2020 Jun), 104787.

[20] P.S. Sen Gupta, S. Biswal, S.K. Panda, A.K. Ray, M.K. Rana, Binding mechanism and structural insights into the identified protein target of COVID-19 and importin-alpha with in-vitro effective drug ivermectin, J. Biomol. Struct. Dyn. 28 (2020 Oct) 1–10.

[21] P.S. Sen Gupta, M.K. Rana, Ivermectin, Famotidine, and Doxycycline: A Suggested Combinatorial Therapeutic for the Treatment of COVID-19, ACS Pharmacol Transl Sci. 3 (5) (2020 Oct 9) 1037–1038.

[22] G. Momekov, D. Momekova, Ivermectin as a potential COVID-19 treatment from the pharmacokinetic point of view: antiviral levels are not likely attainable with known dosing regimens, Biotechnol. Biotechnol. Equip. 34 (1) (2020) 469–474.

[23] C. Chaccour, F. Hammann, S. Ramon-Garcia, N.R. Rabinovich, Ivermectin and COVID-19: Keeping Rigor in Times of Urgency, Am. J. Trop. Med. Hyg. 102 (6) (2020 Jun) 1156–1157.

[24] C.A. Guzzo, C.I. Furtek, A.G. Porras, C. Chen, R. Tipping, C.M. Clineschmidt, et al., Safety, tolerability, and pharmacokinetics of escalating high doses of ivermectin in healthy adult subjects, J. Clin. Pharmacol. 42 (10) (2002 Oct) 1122–1133.

[25] INCHEM. Ivermectin. 2020 [cited 2020 7/9/2020]; Available from: http://www.inchem.org/documents/pims/pharm/ivermect.htm.

[26] Merck Sharp Dohme. Product information for AusPAR Stromectol Ivermectin. 2013.

[27] U. Arshad, H. Pertinez, H. Box, L. Tatham, R.K.R. Rajoli, P. Curley, et al., Prioritization of Anti-SARS-Cov-2 Drug Repurposing Opportunities Based on Plasma and Target Site Concentrations Derived from their Established Human Pharmacokinetics, Clin. Pharmacol. Ther. 108 (4) (2020 Oct) 775–790.

[28] V.D. Schmith, J. Zhou, L.R. Lohmer, The Approved Dose of Ivermectin Alone is not the Ideal Dose for the Treatment of COVID-19, Clin. Pharmacol. Ther. (2020).

[29] R. Zhang, Y. Dong, M. Sun, Y. Wang, C. Cai, Y. Zeng, et al., Tumor-associated inflammatory microenvironment in non-small cell lung cancer: correlation with FGFR1 and TLR4 expression via PI3K/Akt pathway, J Cancer. 10 (4) (2019) 1004–1012.

[30] Y. Javadzadeh, S. Yaqoubi, in: Therapeutic nanostructures for pulmonary drug delivery. Nanostructures for Drug Delivery, Elsevier, 2017, pp. 619–638.

[31] A.A. Mahmoud, N.A. Elkasabgy, A.A. Abdelkhalek, Design and characterization of emulsified spray dried alginate microparticles as a carrier for the dually acting drug roflumilast, Eur. J. Pharm. Sci. 15 (122) (2018 Sep) 64–76.

[32] C.M. Fernandes, M. Teresa Vieira, F.J. Veiga, Physicochemical characterization and in vitro dissolution behavior of nicardipine-cyclodextrins inclusion compounds, Eur. J. Pharm. Sci. 15 (1) (2002 Feb) 79–88.

[33] R.F. Vianna, M.V.L. Bentley, G. Ribeiro, F.S. Carvalho, A.F. Neto, D.C. de Oliveira, et al., Formation of cyclodextrin inclusion complexes with corticosteroids: their characterization and stability, Int. J. Pharm. 167 (1–2) (1998) 205–213.

[34] S.I.F. Badawy, M.M. Ghorab, C.M. Adeyeye, Characterization and bioavailability of danazol-hydroxypropyl β-cyclodextrin coprecipitates, Int. J. Pharm. 128 (1–2) (1996) 45–54.

[35] A. Maged, A.A. Mahmoud, M.M. Ghorab, Nano Spray Drying Technique as a Novel Approach To Formulate Stable Econazole Nitrate Nanosuspension Formulations for Ocular Use, Mol. Pharm. 13 (9) (2016 Sep 06) 2951–2965.

[36] A. Maged, A.A. Mahmoud, M.M. Ghorab, Hydroxypropyl-beta-cyclodextrin as cryoprotectant in nanoparticles prepared by nano-spray drying technique, J. Pharm. Sci. Emerg. Drugs 5 (1) (2017) doi:10.4172/2380-9477.1000121.

[37] T. Serno, R. Geidobler, G. Winter, Protein stabilization by cyclodextrins in the liquid and dried state, Adv. Drug Deliv. Rev. 63 (13) (2011 Oct) 1086–1106.

[38] S. Tavornvipas, S. Tajiri, F. Hirayama, H. Arima, K. Uekama, Effects of hydrophilic cyclodextrins on aggregation of recombinant human growth hormone, Pharm. Res. 21 (12) (2004 Dec) 2369–2376.

[39] Z. Shao, R. Krishnamoorthy, A.K. Mitra, Cyclodextrins as nasal absorption promoters of insulin: mechanistic evaluations, Pharm. Res. 9 (9) (1992 Sep) 1157–1163.

[40] F. Taneri, T. Güneri, M. Kata, Improvement in the physicochemical properties of ketoconazole through complexation with cyclodextrin derivatives, J Incl Macrocycl Chem. 44 (1) (2002) 257–260.

[41] H.M.C. Marques, J. Hadgraft, I.W. Kellaway, G. Taylor, Studies of cyclodextrin inclusion complexes. IV. The pulmonary absorption of salbutamol from a complex with 2-hydroxypropyl-β-cyclodextrin in rabbits, Int. J. Pharm. 77 (2–3) (1991) 303–307.

[42] M. Guan, X. Zeng, R. Shi, Y. Zheng, W. Fan, W. Su, Aerosolization Performance, Antitussive Effect and Local Toxicity of Naringenin-Hydroxypropyl-beta-Cyclodextrin Inhalation Solution for Pulmonary Delivery, AAPS PharmSciTech. 22 (1) (2021 Jan 3) 20.

[43] S. Milani, H. Faghihi, A. Roulholamini Najafabadi, M. Amini, H. Montazeri, A. Vatanara, Hydroxypropyl beta cyclodextrin: a water-replacement agent or a surfactant upon spray freeze-drying of IgG with enhanced stability and aerosolization, Drug Dev. Ind. Pharm. 46 (3) (2020) 403–411.

[44] D. Cataldo, B. Evrard, A. Noel, J.-M. Foldart, Inventors; Use of cyclodextrin for treatment and prevention of bronchial inflammatory diseases, 2015.

[45] A. Martin, Physical pharmacy: physical chemical principles in the pharmaceutical sciences: BI Waverly. Pvt Ltd; 1993.

[46] R.H. Walters, B. Bhatnagar, S. Tchessalov, K.-I. Izutsu, K. Tsumoto, S. Ohtake, Next generation drying technologies for pharmaceutical applications, J. Pharm. Sci. 103 (9) (2014) 2673–2695.

[47] Lubrizol CDMO. Lyophilization of Pharmaceuticals: An Overview. 2019; Available from: https://lubrizolcdmo.com/blog/lyophilization-of-pharmaceuticals-an-overview/.

[48] M.M. Doile, K.A. Fortunato, I.C. Schmucker, S.K. Schucko, M.A. Silva, P. O. Rodrigues, Physicochemical properties and dissolution studies of dexamethasone acetate-beta-cyclodextrin inclusion complexes produced by different methods, AAPS PharmSciTech. 9 (1) (2008) 314–321.

[49] WHO. WHO advises that ivermectin only be used to treat COVID-19 within clinical trials. 2021 [cited 2021 July]; Available from: https://www.who.int/news-room/feature-stories/detail/who-advises-that-ivermectin-only-be-used-to-treat-covid-19-within-clinical-trials.

[50] R.A. Shoukri, I.S. Ahmed, R.N. Shamma, In vitro and in vivo evaluation of nimesulide lyophilized orally disintegrating tablets, Eur. J. Pharm. Biopharm. : Off. J. Arbeitsgemeinschaft fur Pharmazeutische Verfahrenstechnik eV [Comparative Study Randomized Controlled Trial]. 73 (1) (2009 Sep) 162–171.

[51] J.E. Phillips, Inhaled efficacious dose translation from rodent to human: A retrospective analysis of clinical standards for respiratory diseases, Pharmacol. Ther. 178 (2017 Oct) 141–147.

[52] S.M. Mansour, H.S. El-Abhar, A.A. Soubh, MiR-200a inversely correlates with Hedgehog and TGF-beta canonical/non-canonical trajectories to orchestrate the anti-fibrotic effect of Tadalafil in a bleomycin-induced pulmonary fibrosis model, Inflammopharmacology 29 (1) (2021 Feb) 167–182.

[53] K.S. Suvarna, C. Layton, J.D. Bancroft, Bancroft's theory and practice of histological techniques E-Book, Elsevier Health Sciences, Oxford, 2018.

[54] L. Yamanel, U. Kaldirim, Y. Oztas, O. Coskun, Y. Poyrazoglu, M. Durusu, et al., Ozone therapy and hyperbaric oxygen treatment in lung injury in septic rats, Int. J. Med. Sci. 8 (1) (2011 Jan 3) 48–55.

[55] H. Kaur, N. Shekhar, S. Sharma, P. Sarma, A. Prakash, B. Medhi, Ivermectin as a potential drug for treatment of COVID-19: an in-sync review with clinical and computational attributes, Pharmacol. Rep. (2021 Jan 3).

[56] F.R. Formiga, R. Leblanc, Reboucas J de Souza, L.P. Farias, R.N. de Oliveira, L. Pena, Ivermectin: an award-winning drug with expected antiviral activity against COVID-19, J. Control. Release 10 (329) (2021 Jan) 758–761.

[57] C. Chaccour, G. Abizanda, A. Irigoyen-Barrio, A. Casellas, A. Aldaz, F. Martinez-Galan, et al., Nebulized ivermectin for COVID-19 and other respiratory diseases, a proof of concept, dose-ranging study in rats, Sci. Rep. 10 (1) (2020 Oct 13) 17073.

[58] N. Mittal, R. Mittal, Inhaled route and anti-inflammatory action of ivermectin: Do they hold promise in fighting against COVID-19? Med. Hypotheses 146 (2021 Jan), 110364.

[59] WHO. Proposal to waive in vivo bioequivalence requirements for the who model list of essential medicines immediate release, solid oral dosage forms. Working document QAS/04109/Rev1. 2005.

[60] Z. Wang, X. Zhang, Y. Deng, T. Wang, Complexation of hydrophobic drugs with hydroxypropyl-β-cyclodextrin by lyophilization using a tertiary butyl alcohol system, J. Incl. Phenom. Macrocycl. Chem. 57 (1) (2007) 349–354.

[61] T. Loftsson, P. Jarho, M. Másson, T. Järvinen, Cyclodextrins in drug delivery, Expert Opinion on Drug Delivery. 2 (2) (2005) 335–351.

[62] P. Saokham, C. Muankaew, P. Jansook, T. Loftsson, Solubility of Cyclodextrins and Drug/Cyclodextrin Complexes, Molecules 23 (5) (2018).

[63] M.E. Brewster, T. Loftsson, Cyclodextrins as pharmaceutical solubilizers, Adv. Drug Deliv. Rev. 59 (7) (2007) 645–666.

[64] R.A. Rajewski, V.J. Stella, Pharmaceutical applications of cyclodextrins. 2. In vivo drug delivery, J. Pharm. Sci. 85 (11) (1996 Nov) 1142–1169.

[65] F. Semcheddine, N.E.I. Guissi, X. Liu, Z. Wu, B. Wang, Effects of the preparation method on the formation of true nimodipine SBE-β-CD/HP-β-CD inclusion complexes and their dissolution rates enhancement, AAPS PharmSciTech. 16 (3) (2015) 704–715.

[66] P. Vass, B. Démuth, A. Farkas, E. Hirsch, E. Szabó, B. Nagy, et al., Continuous alternative to freeze drying: Manufacturing of cyclodextrin-based reconstitution powder from aqueous solution using scaled-up electrospinning, J. Control. Release 298 (2019) 120–127.

[67] M.L. Calabro, S. Tommasini, P. Donato, D. Raneri, R. Stancanelli, P. Ficarra, et al., Effects of alpha- and beta-cyclodextrin complexation on the physico-chemical properties and antioxidant activity of some 3-hydroxyflavones, J. Pharm. Biomed. Anal. [Comparative Study]. 35 (2) (2004 Apr 16) 365–377.

[68] H.O. Ammar, H.A. Salama, M. Ghorab, A.A. Mahmoud, Formulation and biological evaluation of glimepiride-cyclodextrin-polymer systems, Int. J. Pharm. 309 (1–2) (2006 Feb 17) 129–138.

[69] L. Zhang, W. Zhu, Q. Lin, J. Han, L. Jiang, Y. Zhang, Hydroxypropyl-beta-cyclodextrin functionalized calcium carbonate microparticles as a potential carrier for enhancing oral delivery of water-insoluble drugs, Int. J. Nanomed. 10 (2015) 3291–3302.

[70] C.L. Jackson, G.B. McKenna, Vitrification and crystallization of organic liquids confined to nanoscale pores, Chem. Mater. 8 (8) (1996) 2128–2137.

[71] S. Soni, M.R. Wilson, K.P. O'Dea, M. Yoshida, U. Katbeh, S.J. Woods, et al., Alveolar macrophage-derived microvesicles mediate acute lung injury, Thorax 71 (11) (2016 Nov) 1020–1029.

[72] Z. Vitenberga, M. Pilmane, Inflammatory, anti-inflammatory and regulatory cytokines in relatively healthy lung tissue as an essential part of the local immune system, Biomed. Pap. Med. Fac. Univ. Palacky Olomouc Czech Repub. 161 (2) (2017 Jun) 164–173.

[73] D.L. Laskin, R. Malaviya, J.D. Laskin, Role of Macrophages in Acute Lung Injury and Chronic Fibrosis Induced by Pulmonary Toxicants, Toxicol. Sci. 168 (2) (2019 Apr 1) 287–301.

[74] T. Roszer, Understanding the Mysterious M2 Macrophage through Activation Markers and Effector Mechanisms, Mediators Inflamm. 2015 (2015), 816460.

[75] M.G. Chiaramonte, M. Mentink-Kane, B.A. Jacobson, A.W. Cheever, M.J. Whitters, M.E. Goad, et al., Regulation and function of the interleukin 13 receptor alpha 2 during a T helper cell type 2-dominant immune response, J. Exp. Med. 197 (6) (2003 Mar 17) 687–701.

[76] C. Jakubzick, E.S. Choi, B.H. Joshi, M.P. Keane, S.L. Kunkel, R.K. Puri, et al., Therapeutic attenuation of pulmonary fibrosis via targeting of IL-4- and IL-13-responsive cells, J. Immunol. 171 (5) (2003 Sep 1) 2684–2693.

[77] A.J. Santanasto, R.K. Cvejkus, M.K. Wojczynski, M.M. Marron, N. Schupf, K. Christensen, et al., Circulating Procollagen type III N-terminal peptide (P3NP) and Physical Function in Adults from The Long Life Family Study, J. Gerontol. A Biol. Sci. Med. Sci. 14 (2020 Aug).

[78] R.P. Marshall, G. Bellingan, S. Webb, A. Puddicombe, N. Goldsack, R.J. McAnulty, et al., Fibroproliferation occurs early in the acute respiratory distress syndrome and impacts on outcome, Am. J. Respir. Crit. Care Med. 162 (5) (2000 Nov) 1783–1788.

[79] Y. Su, H. Gu, D. Weng, Y. Zhou, Q. Li, F. Zhang, et al., Association of serum levels of laminin, type IV collagen, procollagen III N-terminal peptide, and hyaluronic acid with the progression of interstitial lung disease, Medicine (Baltimore). 96 (18) (2017 May), e6617.

[80] L. Bjermer, R. Lundgren, R. Hallgren, Hyaluronan and type III procollagen peptide concentrations in bronchoalveolar lavage fluid in idiopathic pulmonary fibrosis, Thorax 44 (2) (1989 Feb) 126–131.

[81] S. Awasthi, J.J. Coalson, B.A. Yoder, E. Crouch, R.J. King, Deficiencies in lung surfactant proteins A and D are associated with lung infection in very premature neonatal baboons, Am. J. Respir. Crit. Care Med. 163 (2) (2001 Feb) 389–397.

[82] Z. Lin, C. Pearson, V. Chinchilli, S.M. Pietschmann, J. Luo, U. Pison, et al., Polymorphisms of human SP-A, SP-B, and SP-D genes: association of SP-B Thr131Ile with ARDS, Clin. Genet. 58 (3) (2000 Sep) 181–191.

[83] T.R. Korfhagen, Surfactant protein A (SP-A)-mediated bacterial clearance: SP-A and cystic fibrosis, Am. J. Respir. Cell Mol. Biol. 25 (6) (2001 Dec) 668–672.

[84] Y. Kuroki, S. Tsutahara, N. Shijubo, H. Takahashi, M. Shiratori, A. Hattori, et al., Elevated levels of lung surfactant protein A in sera from patients with idiopathic pulmonary fibrosis and pulmonary alveolar proteinosis, Am. Rev. Respir. Dis. 147 (3) (1993 Mar) 723–729.

[85] R. Sumagin, E. Lomakina, I.H. Sarelius, Leukocyte-endothelial cell interactions are linked to vascular permeability via ICAM-1-mediated signaling, Am. J. Physiol. Heart Circ. Physiol. 295 (3) (2008 Sep) H969–H977.

[86] M.D. Bird, M.O. Morgan, L. Ramirez, S. Yong, E.J. Kovacs, Decreased pulmonary inflammation after ethanol exposure and burn injury in intercellular adhesion molecule-1 knockout mice, J. Burn Care Res. 31 (4) (2010 Jul-Aug) 652–660.

[87] S. Montefort, W.R. Roche, P.H. Howarth, R. Djukanovic, C. Gratziou, M. Carroll, et al., Intercellular adhesion molecule-1 (ICAM-1) and endothelial leucocyte adhesion molecule-1 (ELAM-1) expression in the bronchial mucosa of normal and asthmatic subjects, Eur. Respir. J. 5 (7) (1992 Jul) 815–823.

[88] H. Jiang, R.M. Klein, D. Niederacher, M. Du, R. Marx, M. Horlitz, et al., C/T polymorphism of the intercellular adhesion molecule-1 gene (exon 6, codon 469). A risk factor for coronary heart disease and myocardial infarction, Int. J. Cardiol. 84 (2–3) (2002 Aug) 171–177.

[89] D.E. Hallahan, L. Geng, Y. Shyr, Effects of intercellular adhesion molecule 1 (ICAM-1) null mutation on radiation-induced pulmonary fibrosis and respiratory insufficiency in mice, J. Natl Cancer Inst. 94 (10) (2002 May 15) 733–741.
[90] A. Yadav, V. Saini, S. Arora, MCP-1: chemoattractant with a role beyond immunity: a review, Clin. Chim. Acta 411 (21–22) (2010 Nov 11) 1570–1579.
[91] J. Panee, Monocyte Chemoattractant Protein 1 (MCP-1) in obesity and diabetes, Cytokine 60 (1) (2012 Oct) 1–12.
[92] J.N. Hilda, S.D. Das, TLR stimulation of human neutrophils lead to increased release of MCP-1, MIP-1alpha, IL-1beta, IL-8 and TNF during tuberculosis, Hum. Immunol. 77 (1) (2016 Jan) 63–67.
[93] S. Al-Mazidi, M. Alotaibi, T. Nedjadi, A. Chaudhary, M. Alzoghaibi, L. Djouhri, Blocking of cytokines signalling attenuates evoked and spontaneous neuropathic pain behaviours in the paclitaxel rat model of chemotherapy-induced neuropathy, Eur. J. Pain 22 (4) (2018 Apr) 810–821.
[94] S. Thibaut de Menonville, C. Rosignoli, E. Soares, M. Roquet, B. Bertino, J. P. Chappuis, et al., Topical Treatment of Rosacea with Ivermectin Inhibits Gene Expression of Cathelicidin Innate Immune Mediators, LL-37 and KLK5, in Reconstructed and Ex Vivo Skin Models, Dermatol Ther (Heidelb) 7 (2) (2017 Jun) 213–225.
[95] C.J. Lechner, R.G. Gantin, T. Seeger, A. Sarnecka, J. Portillo, H. Schulz-Key, et al., Chemokines and cytokines in patients with an occult Onchocerca volvulus infection, Microbes Infect. 14 (5) (2012 May) 438–446.